Unexpectedly High Yield Carbon Nanotube Synthesis from Low-Activity Carbon Feedstocks at High Concentrations

Hiroe Kimura,[†,§] Jundai Goto,[†] Satoshi Yasuda,[†] Shunsuke Sakurai,[†] Motoo Yumura,[†] Don N. Futaba,[†,*] and Kenji Hata[†,‡,§,*]

[†]Nanotube Research Center, National Institute of Advanced Industrial Science and Technology (AIST), Tsukuba, 305-8565, Japan, [‡]Japan Science and Technology Agency (JST), Kawaguchi, 332-0012, Japan, and [§]Department of Pure and Applied Sciences, Tsukuba University, Tsukuba, 305-8573, Japan

ABSTRACT We report a new direction for highly efficient carbon nanotube (CNT) synthesis where, in place of conventional highly reactive carbon feedstocks at low concentrations, highly stable carbon feedstocks at high concentrations were shown to produce superior yields. We found that a saturated hydrocarbon that is considered to possess a low reactivity, delivered at high concentrations, could achieve an extremely high growth yield (2.5 times that when using ethylene). This result stems from the unique behavior where the CNT yield linearly increased with carbon concentration, in contrast to more reactive carbon feedstocks, where the yield peaks. We propose that the mechanisms for the growth kinetics for high- and low-reactivity carbon feedstocks are fundamentally different, where the latter benefits from a longer catalyst lifetime because of a relatively low production rate of carbon impurities.

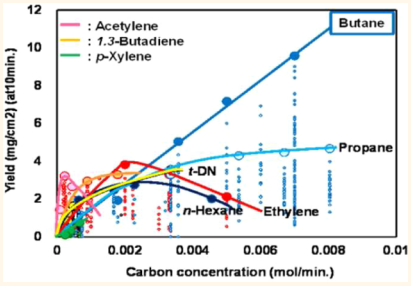

KEYWORDS: carbon nanotube · single-walled carbon nanotube · CNT · SWCNT · SWNT · carbon feedstocks

The synthesis of carbon nanotubes (CNTs) has always represented one of the main obstacles for scientific research and industrial applications. To address this point, extensive research has been focused to control both the growth structure and to improve the CNT growth efficiency, *e.g.*, yield,[1−8] crystallinity,[9−13] and chirality.[14,15] Examples include the water-assisted chemical vapor deposition method to increase yield,[2] the floating catalyst chemical vapor deposition (CVD) method to improve crystallinity,[11] and catalyst gas pretreatments for metal conductor selective growth.[14,15]

Typically, in the CVD synthetic process of CNTs, hydrocarbon gases are used as carbon feedstocks. It is well recognized that the choice of carbon feedstock is a crucial factor in achieving the desired synthesis, and thus the synthesis of CNTs has been developed using a wide variety of hydrocarbons, including methane,[16,17,19] acetylene,[16,22,23] ethylene,[2,16] and anthracene.[17] Particularly, the choice of the carbon feedstock has been reported to have great consequences on the carbon nanotube structure and yield.[1−8,16−18,21] For example, a number of reports have demonstrated a clear effect of the CNT structure on the choice of carbon feedstock and have found a clear trend in single-walled carbon nanotube (SWCNT) and multiwalled carbon nanotube (MWCNT) formation.[16−18] Furthermore, through the development of CNT synthesis by the CVD method, the carbon feedstock and process were the direct approach to overcome the obstacles of low purity, low yield, and single-wall selectivity. A methane growth ambient was first used to demonstrate the synthesis of carbon nanotubes by a CVD process.[19] To improve all three properties, a carbon monoxide carbon feedstock was utilized at high pressure, well known as the HiPco process, which realized one of the first mass productions of SWCNTs with high selectivity.[20] Similarly, carbon feedstocks containing oxygen, alcohols, dramatically increased the yield of SWCNTs and realized the first vertically standing SWCNTs with a height of

* Address correspondence to kenji-hata@aist.go.jp; d-futaba@aist.go.jp.

Received for review November 28, 2012 and accepted March 4, 2013.

Published online March 04, 2013
10.1021/nn305513e

4 μm.[21] Among all the hydrocarbons used for CNT synthesis, most commonly, unsaturated chain hydrocarbons have been used, such as acetylene because of the high reactivity and ability to produce CNTs in high yield. Eres *et al.*[22] reported through molecular beam-controlled nucleation experiments that acetylene exhibited an order of magnitude higher efficiency in forming the carbon network. Additionally, Zhong *et al.* reported that acetylene was the primary component in CNT growth,[23] and Bronkowski *et al.* reported that acetylene possessed an exceptionally low activation energy.[24] In fact, only with acetylene has highly efficient forest growth, that is, millimeter-tall forests in ~10 min, been made possible. For other carbon feedstocks, such as ethylene, water is required to achieve similarly high yields.[25] These studies suggest that acetylene is currently the best choice for CNT synthesis.

When a carbon feedstock is delivered into the reaction chamber of a CVD system, the concentration is a critical parameter because for a given growth process (*i.e.*, flow rate, temperature, catalyst composition, catalyst amount) an optimum carbon feedstock concentration exists for the yield. In general, it is well known that as the carbon feedstock concentration increases, the yield increases, peaks, and then drops. This is because at low feedstock concentrations, the rate-limiting step is the supply of carbon; therefore, as the feedstock concentration increases, the CNT yield also increases. At the peak, the carbon concentration and ability of the catalysts to convert the feedstock to CNTs are balanced. As the feedstock concentration increases beyond the optimum level, the rate-limiting step shifts to the ability of the available catalysts to convert the carbon into CNTs; thus catalyst deactivation through carbon coating occurs more quickly, and the yield drops with further increase. Specifically, the catalyst lifetime is shortened. A significant advantage of acetylene is the ability to produce a high yield of CNTs while using only a low feedstock concentration. As previously mentioned, this stems from the high efficiency of the acetylene feedstock and its important synthetic role in CNT synthesis. However, when a growth enhancer is added at even ~100 ppm levels, this optimum carbon concentration can be greatly increased,[2,26] which leads to a dramatic increase in growth yield, as exemplified by water-assisted CVD (Supergrowth method). This shift results from the suppression of the deactivation process, and hence, the catalysts can survive at even high carbon feedstock concentrations.[27] Without water, at a ethylene concentration as low as 1%, the lifetime of the catalysts is only ~1 min, but when water is introduced, the lifetime can be extended beyond >30 min. In this manner, the yield can be increased 1000-fold; however, despite the addition of water, a peak still exists, beyond which the catalysts deactivate and the growth declines. Therefore, the current trend for CNT synthesis is the use of highly active carbon feedstocks at low concentrations.

In this paper, we report an entirely different approach where, in contrast to using highly active carbon feedstocks at low concentrations, low-activity carbon feedstocks are used at high concentrations, exceeding the saturation concentrations for active sources, to achieve unprecedented and superior CNT growth yields. We found that when an unsaturated chain hydrocarbon, such as butane, was used as the carbon feedstock, the yield linearly increased with concentration and did not show saturation or a peak as observed with the other groups of hydrocarbons. As a result, we could achieve a 2.5-fold higher optimum growth yield than that using ethylene. We propose that the mechanisms for the growth kinetics between high- and low-reactivity carbon feedstocks are fundamentally different, where the latter benefits from a longer catalyst lifetime because of a relatively low production rate of carbon impurities.

RESULTS AND DISCUSSION

Unique to this study, we chose the carbon feedstock concentration, an experimental parameter that had been neglected in most previous growth studies, as the principle parameter. This is because we found that growth yield greatly depended on this parameter, while most previous growth studies have intensively studied the effect of other growth parameters, such as growth temperature, growth time, and water level. Water-assisted CVD was used as a representative CVD method because, as mentioned previously, the use of water (or growth enhancer) shifted the usable feedstock concentrations to allow higher levels and produce higher (and measurable) growth yields. In short, synthesis was carried out at 750 °C on a 1 in. tube furnace with He and H_2 carrier gases with ethylene as a carbon source at a total flow of 500 sccm with a sputtered Fe/Al_2O_3 catalyst (1.5/40 nm) (for details, please see Methods). The three input parameters of water-assisted CVD were the water level, growth temperature, and carbon feedstock concentration. To examine the empirical relationship of carbon concentration on the growth yield, we plotted the CNT yield as a function of carbon concentration using an ethylene carbon feedstock (Figure 1a). For a fixed ethylene concentration, the growth temperature (700−900 °C) and water level were sequentially optimized to optimize yield. This required ~36 growths at a specific ethylene concentration. This process was repeated for five different ethylene concentrations spanning 0.0004 to 0.005 mol/min (1−12% or 5−60 sccm at a total flow of 500 sccm). After ~200 growths, the global and local maxima in the growth yield, as well as the relationship with the ethylene concentration, were found. Figure 1a represents the cumulative optimization results for

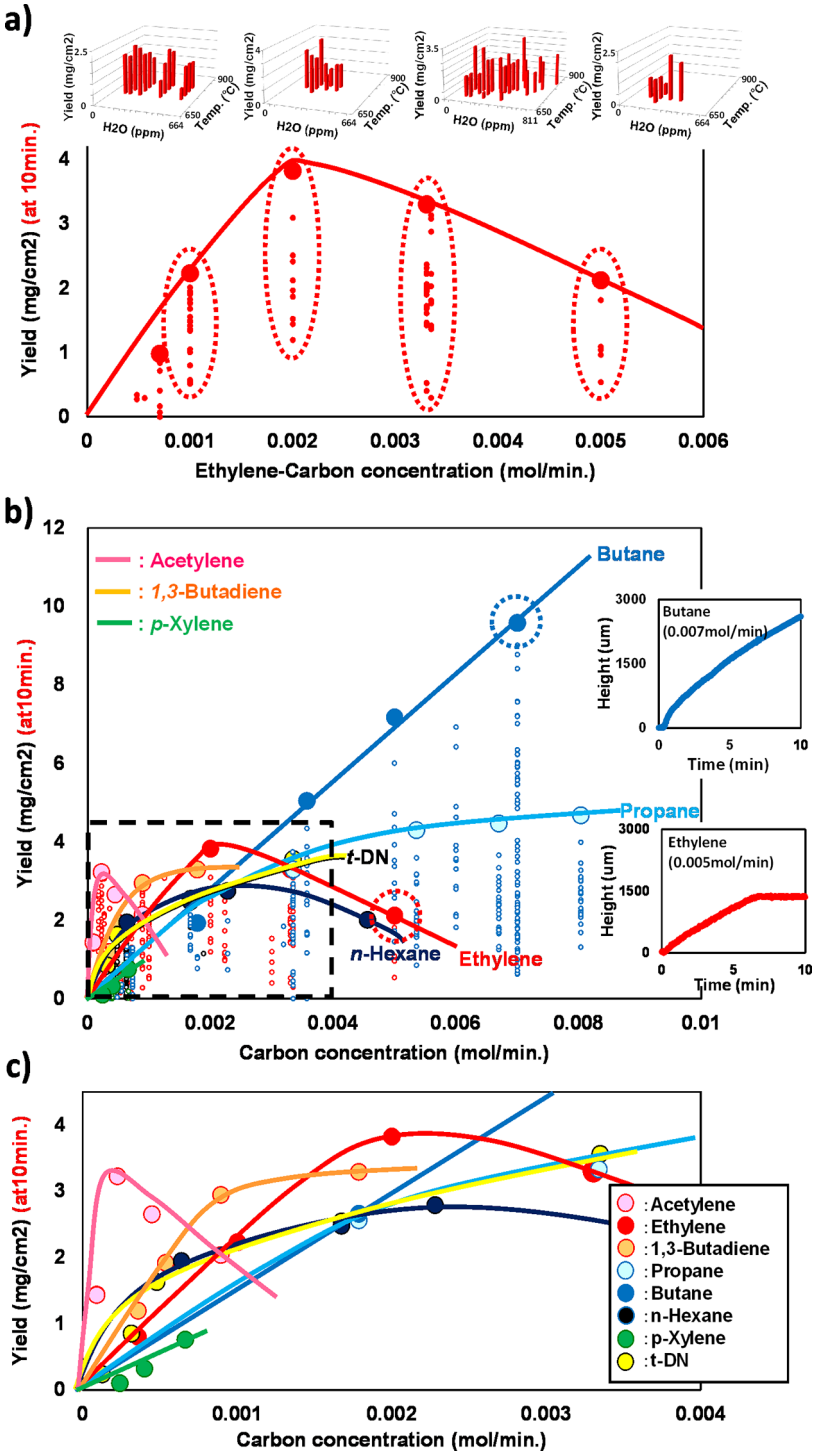

Figure 1. Relation of the optimized yield as a function of carbon feedstock concentration. (a) Optimized CNT yields as a function of ethylene concentration. Large dots represent the optimized value at each concentration. (Inset: 2D plots of the yield as a function of water concentration and temperature for selected points.) (b) Optimized yields for various carbon feedstocks (line are added to guide the eye). (Upper inset: CNT growth evolution plot for butane for selected point. Lower inset: CNT growth evolution plot for ethylene for selected point.) (c) Enlarged graph of panel (b) to discriminate the trends of the carbon feedstocks at low concentrations.

ethylene where the local maximum at each carbon concentration is marked by a large dot and the general trend is highlighted by a solid line. The inset figures are three-dimensional plots of the yield as functions of water level and growth temperature to emphasize the optimization results for a single ethylene concentration. As the ethylene concentration increased, the yield rose sharply, which then peaked at ~4 mg/cm^2 when the ethylene concentration reached ~0.0020 mol/min. As the ethylene concentration increased beyond this

value, the yield then steadily declined. This is a well-known behavior of the yield with the carbon feedstock concentration with or without water. We extended this procedure to encompass the broadest set of hydrocarbon feedstocks: saturated rings, saturated chains, unsaturated and aromatic rings, and unsaturated chains. Specifically, this included *trans*-decahydronaphthalene (*t*-DN), *para*-xylene (*p*-xylene), propane, butane, *n*-hexane, 1,3-butadiene, ethylene, and acetylene. We repeated the entire synthesis optimization process for the eight carbon feedstocks to investigate other avenues for high-yield CNT synthesis beyond highly reactive carbon feedstocks. As a whole, this encompassed ~2000 total synthesis processes. We would like to note that the growth conditions (catalyst formation temperature and total gas flow) were fixed.

Central to this work, we found a trend unreported in the literature where, in the high carbon concentration regime, unsaturated chain hydrocarbons, such as butane, could provide a much higher yield than the commonly used carbon feedstocks, such as acetylene and ethylene. A detailed structural characterization of the SWCNT forests grown from each carbon feedstock showed a similar diameter, wall number, and purity,[28] but the growth kinetics significantly differed. Furthermore, we found that within our synthetic system the catalyst determined most aspects of the CNT forest structure, such as diameter and bulk density, and only the yield was determined by the carbon feedstock.[28] Therefore in this paper, we focused on the aspects of growth kinetics. In general, the trends for the yield for all carbon feedstocks were similar to ethylene, where the yield exhibited a rise, peak, and decline as the carbon feedstock concentration increased (Figure 1b,c). Butane and propane were the exceptions to this general rule, where they did not exhibit a peak even at our highest carbon feedstock concentrations (Figure 1b). Specifically, for butane, the yield, as quantified as the weight per substrate area for a fixed growth time, increased from ~1.3 mg/cm^2 (~300 μm height) at 0.0007 mol/min to as high as ~9.6 mg/cm^2 (2400 μm height) at 0.007 mol/min. This was over double the highest reported yield using other carbon feedstocks, such as acetylene and ethylene. While we do not discount the existence of a peak for butane, it is clear that the peaking level would be located in a vastly higher region if it exists. Experimentally, it is difficult to address the higher concentration levels, as the carbon feedstock decomposes and creates a thick smoke of gaseous tar. In fact, with increased carbon concentration, the CNT yield using butane linearly increased within our experimental limits. The growth evolution curve was measured by an *in situ* telecentric height monitoring system, which provides real-time height monitoring of nanotube forests using the projected shadow of the forest created from a parallel green light

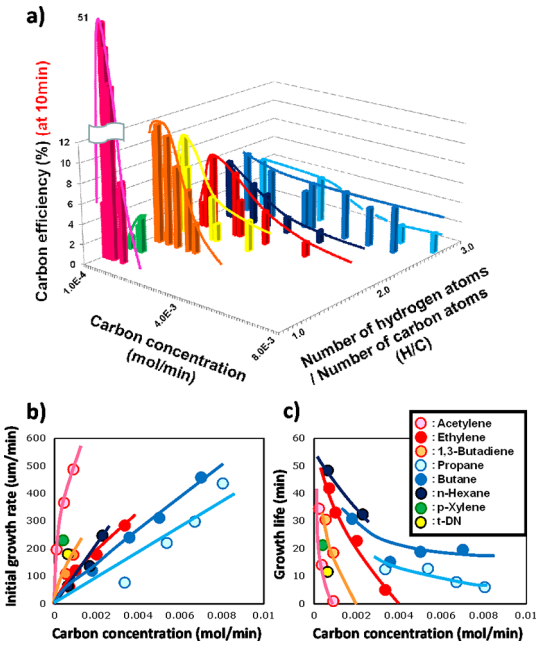

Figure 2. Characterization of the CNT growth for each carbon feedstock. (a) Calculated carbon efficiency as a function of the carbon concentration and hydrogen-to-carbon ratio, Calculated (b) initial growth rates and (c) growth lifetimes of the CNT forests as a function of the carbon concentration. (Lines are added to guide the eye.)

flow focused onto a CCD through a telecentric optical system.[29] The growth evolution curve of the forest for butane feedstock (indicated by the dotted circle) showed continued growth over the 10 min growth span without growth termination or saturation (Figure 1b, upper inset). The linearity of the growth evolution curve and the linearity of the yield indicate that the calculated yield was not a result of carbon impurity accumulation.[30] In contrast to unsaturated hydrocarbons (Figure 1b (lower inset)), saturated hydrocarbons at high carbon feedstock concentrations could produce high CNT yield. This means that within a certain growth time, butane can produce the highest yield of CNTs, which is a significant advantage of SWCNT forest synthesis.

To gain deeper insight into these observed trends, we plotted the carbon efficiency as a function of carbon feedstock concentration and the ratio of hydrogen to carbon atoms within each hydrocarbon species (Figure 2a). Carbon efficiency was defined as the percentage of the input carbon feedstock that is converted to SWCNTs and was estimated by the quotient of masses of synthesized SWCNT forest and input carbon (multiplied by 100). We grouped the hydrocarbon species as the ratio of hydrogen to carbon atoms as an indicator of saturation. For example, for unsaturated hydrocarbons this ratio would be small (acetylene: 1), and for fully saturated hydrocarbons this ratio would be large (propane: 2.7). From this plot, we made several observations. In agreement with previous observations, highly unsaturated hydrocarbons

(*e.g.*, acetylene, ethylene) exhibited the highest carbon efficiencies (as high as ~51%). We believe this feature was the reason that acetylene and ethylene have been the choice for many CVD studies. Further, for unsaturated hydrocarbons, as exemplified by acetylene, as the carbon concentration increased, the carbon efficiency sharply rose, peaked, and sharply dropped. It is interesting to note that *p*-xylene, despite also being an unsaturated hydrocarbon, exhibited poor carbon efficiency, highlighting the contribution of the aromatic structure to the growth properties. This behavior was observed for all groups of carbon feedstocks with the exception of highly saturated hydrocarbons (butane, propane). In contrast, the highly saturated hydrocarbons showed lower carbon efficiencies (~4.5−6.1%) at similar carbon concentrations, but the behavior with carbon concentration was drastically different. As opposed to exhibiting a sharp peak, highly saturated hydrocarbon feedstocks, such as butane, showed an exceptionally flat profile with increasing carbon concentration. In fact, for butane the carbon efficiency dropped only 23% across our entire experimental range, whereas acetylene and other saturated hydrocarbons dropped nearly ~100%. To highlight the stark difference at high concentrations, at a carbon feedstock concentration of 11%, the butane carbon efficiency was ~4.6% as compared with ~0% for acetylene. The carbon efficiency of butane far exceeded those of unsaturated hydrocarbons at these high concentrations, which suggests different growth kinetics.

To gain deeper insight into the difference in the growth kinetics, we measured the height evolution of the SWCNT forest curves by an *in situ* telecentric height monitoring system for each of the hydrocarbons for each of the growth conditions. The wide dynamic range (up to 1 cm) with high resolution (1 um) of the monitoring system enabled our study of the SWCNT forest heights, short (<100 μm) or tall (>2500 μm), with great accuracy. For each measurement, the height of the forest was measured continuously and formed a growth evolution curve, such as the insets of Figure 1b. According to first-order kinetics, the growth equation of the height (yield) of the forest was described as $H(t) = \beta\tau_o(1 - e^{-t/\tau_o})$, where H is the forest height and the two fitting parameters, β and τ_o, represent the initial growth rate (IGR) and lifetime, respectively.[26] By fitting each growth curve of Figure 1b to this growth equation, the IGR and the catalyst lifetime, which characterized the evolution of the growth, were plotted as a function of carbon concentration (Figure 2b,c). As previously shown for the case of ethylene,[26] a general trend was observed for almost all carbon feedstocks where an inverse relation between the growth rate and lifetime as the carbon feedstock arose as the carbon concentration increased. Specifically, within a carbon concentration range extending from 0.000 09 to ~0.004 mol/min, the growth rates for most carbon

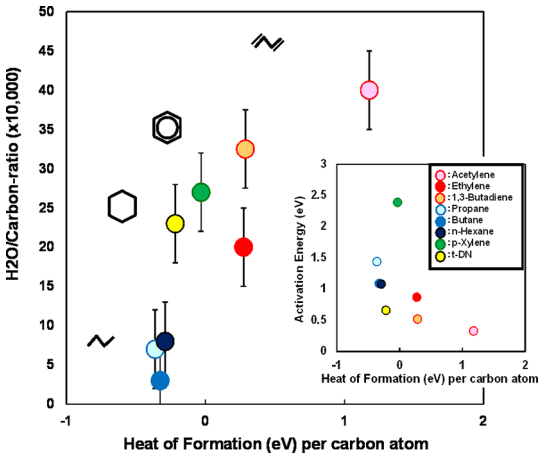

Figure 3. H_2O/carbon ratio as a function of heat of formation (inset: calculated activation energies as a function of heat of formation).

feedstocks rose to as high as 500 μm/min. However, within this same span, the growth lifetimes dramatically dropped from ~50 min to ≪1 min. This explains why we observed a peak in the growth yield for most carbon feedstocks (Figure 1b). In general, butane and propane showed a similar overall trend; that is, the IGR increased while the lifetime decreased with increased carbon concentration. However, at high concentration levels, the growth lifetime of butane showed a weaker dependency on the carbon concentration and thus exhibited only a ~40% decrease. Therefore, the yield exhibited an increase because the catalysts were active throughout the growth period. This explains the continued increase in the yield for butane (Figure 1b) and the constant carbon efficiency (Figure 2a). It should be noted that *n*-hexane exhibited a sharp drop in catalyst lifetime similar to acetylene and ethylene but, in contrast, within the same range did not approach zero, which is similar to its category (butane, propane). While we do not fully understand the uniqueness of butane, we would expect that differences, including its size and cracking pattern, would play a significant role.

To derive a possible mechanism behind the dependency of the growth yield on the carbon feedstock concentration among the various hydrocarbon sources, we plotted the optimized water/carbon feedstock ratio (H_2O/C ratio) as a function of the heat of formation per atom for each feedstock (Figure 3). These values were taken from the growth conditions (optimum growth temperature, optimum water level, and optimum carbon concentration) at optimum yield. The optimum H_2O/C ratio is a crucial value that describes the kinetics of water-assisted SWCNT forest growth. The optimum H_2O/C ratio determines the amount of carbon and water molecules that can be consumed before catalyst deactivation.[26] Furthermore, this H_2O/C ratio is linked to the heat of formation and activation energy of the carbon feedstock. The heat of formation, as opposed to the H/C ratio, is an indicator of molecular stability

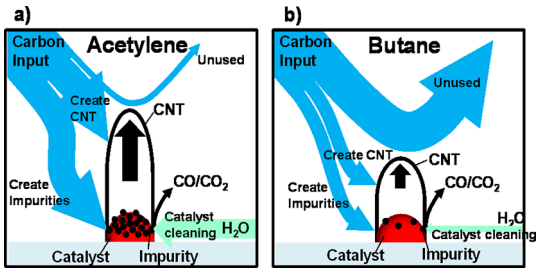

Figure 4. Proposed interpretation of the differing rate-limiting steps for the different carbon feedstocks: CNT growth, impurity formation, and unused, and the use of water to clean the carbon impurities. (a) Condition for high-reactivity carbon feedstocks, such as acetylene. (b) Condition for low-reactivity carbon feedstocks, such as butane.

(or reactivity) and was normalized to account for the number of carbon atoms within each feedstock molecule. From this plot, we made several observations: First, all data fell approximately along a line proportional to the heats of formation. This result indicated that feedstocks with higher formation energies (*i.e.*, reactivities) required higher H_2O/C ratios, which illustrated the need of water to clean the catalyst surface to maintain activity.[26] In fact, acetylene exhibited a 10 times higher H_2O/C ratio than butane. Second, the carbon feedstocks increased in formation energy by hydrocarbon category: saturated chains, saturated rings, unsaturated rings, and unsaturated chains. Third, these results agreed with the trend for the estimated activation energies, where it decreased with increased formation energy (Figure 3, inset).

From these results, we propose a mechanism for the synthesis of CNTs that can explain the observed behavior among the various carbon feedstocks including butane (Figure 4). For the growth model, we adopted the following scheme describing the process of water-assisted CVD. In this model, two competing reactions occur: (1) the production of CNTs and carbon impurities from the exposure of catalyst to heat and carbon and (2) the cleaning of catalysts (*i.e.*, removal of carbon impurities) from the exposure to water.[27] From this model, we interpret that the rate-limiting step in the synthesis of SWNTs from saturated hydrocarbons (*e.g.*, butane) and unsaturated hydrocarbons (*e.g.*, acetylene) is different. From our experimental results, higher reactivity (and lower activation energy) carbon feedstocks, such as unsaturated hydrocarbons, exhibited higher H_2O/C ratios, which would suggest a higher production rate of carbon impurities (a source of catalyst deactivation) (Figure 3).[27] In contrast, lower reactivity carbon feedstocks, particularly as observed with saturated chain hydrocarbons, exhibited lower optimum H_2O/C ratios, which suggest a relatively lower production rate of carbon impurities. (It should be noted that when considering the carbon efficiency in this comparison, this difference in the required H_2O increased 10-fold.) In addition, our results showed that for unsaturated hydrocarbon feedstocks long growth lifetimes could be achieved only at low carbon concentrations where the initial growth rate was low, which limits the optimum achievable yields (Figure 2b,c). In contrast, saturated hydrocarbon feedstocks exhibited long growth lifetimes at high carbon concentrations where the initial growth rates were highest (Figure 2b,c). Therefore, we interpret that, in the case of unsaturated hydrocarbons, such as acetylene, the rate-limiting step was the cleaning of the catalyst surface, which explained the higher optimum H_2O/C ratio and shortened growth lifetime with increased carbon concentration (Figure 4a). It should be noted that, as reported previously, increasing the water content to further aid in the cleaning process leads to a drop in the growth efficiency through catalyst poisoning.[26] In contrast, for butane, we propose that a chemical pathway, different from that of acetylene, occurs that produces carbon impurities at a lower rate. In this case, for butane the rate-limiting step in the synthesis of CNTs would be the conversion process of butane to CNTs (Figure 4b). This mechanism was supported by the experimental result that showed the carbon efficiency to be relatively constant with respect to the feedstock concentration (Figure 2a). This explains the observed lower optimum H_2O/C ratio and the longer growth lifetimes at high carbon concentrations. Finally, this difference in the rate-limiting steps in the synthesis of SWNTs from saturated hydrocarbons (*e.g.*, butane) and unsaturated hydrocarbons (*e.g.*, acetylene) explains why no peak was observed in the yield with increased carbon feedstock concentration (Figure 1b). We would also like to note that we do recognize that the carbon feedstocks can undergo decomposition in the gas phase prior to contact with the catalyst; therefore, our conclusions are not meant to encompass the actual form of the carbon feedstock contributing to CNT synthesis. To fully understand the fundamental chemical reaction(s) involved, molecular dynamic simulations would be required, and we hope that this work invokes future investigation.

SUMMARY

In summary, we have demonstrated a new direction for highly efficient CNT synthesis where, in place of conventional highly reactive carbon feedstocks at low concentration, highly stable carbon feedstocks at high concentrations were shown to produce superior yields. Particularly, we found that butane, a saturated hydrocarbon, showed vastly different behavior from other carbon feedstocks (*e.g.*, acetylene, ethylene) in that the CNT yield linearly increased with carbon flow rate devoid of saturation or a peak within our experimental range. Our proposed mechanism suggests that differing chemical reactions may be occurring for the two carbon feedstocks, which would be an interesting topic of study for simulation or *in situ* TEM. These results are

intended to demonstrate new avenues for high-yield CNT growth beyond conventionally available methods. From a practical aspect, these results also mean that within an arbitrary growth time butane can produce the highest yield of CNTs. This point would be important toward mass production because the Supergrowth process has been[32] scaled-up where continuous CVD on 50 × 50 cm substrates has been realized by the development a belt conveyor, multizone (temperature raising, reduction, growth, and cooling) furnace, CVD system. Finally, as demonstrated, water-assisted CVD can be performed from numerous carbon sources and growth enhancers, which could result in structural control (SW and DWCNT synthesis), high yield, *etc.*, which opens a great number of opportunities.[2,32−34]

METHODS

SWCNT Synthesis. We used a standard Al_2O_3/Fe catalyst (40 nm/1.5 nm) prepared by sputtering that was well established to grow SWCNT forests with high yield. All syntheses were performed using a 1 in. fully automated CVD system equipped with an exchange chamber to enable the numerous (~2000) required syntheses with a controlled and stable ambient. In the standard Supergrowth process, SWCNT forests were synthesized with a C_2H_4 carbon feedstock (~25 sccm), water (50 to 500 ppm), growth enhancer, and He as a carrier gas (total flow: 500 sccm) with a growth time of 10 min. Formation of nanoparticles for all cases was performed at the same conditions, 1:9 He/H_2 and at a temperature of 750 °C, to eliminate the catalyst formation step as a variable. Then the temperature was adjusted to the growth temperature ranging from 725 to 900 °C. The growth temperature and water level were optimized at a fixed specific hydrocarbon flow rate (for highly active feedstocks, the flow rate was intentionally lowered). Carbon feedstock purities: ethylene, 99.999%; acetylene (10% diluted with He), C_2H_2, 99.99%; He, 99.999%; 1,3-butadiene, 99%; propane, 99.99%; *n*-butane:, 99.95%; *n*-hexane, 96%; t-DN, 99%; *p*-xylene, 98%.

Liquid Carbon Feedstock Injection. The liquid carbon sources were introduced using a syringe pump setup with a capillary (100 μm i.d.) input port. The line was preheated before injecting into the growth ambient to ensure that vaporization of the liquid source occurred prior to the growth ambient.

Calculation of Carbon Input Level. For gas sources, the carbon input rate was calculated from the direct conversion of the gas flow rate [sccm] to mol/min as displayed below:

$$\text{eth. concentration [mol/min]} = \text{flow rate [sccm]} \times \left(\frac{1\ \text{L}}{1000\ \text{cm}^3}\right)\left(\frac{P}{RT}\right)\left(\frac{2\ \text{mol carbon}}{1\ \text{mol ethylene}}\right)$$

where P is the pressure (1 atm), R is the gas constant (0.082 L/atm·mol·K), and T is the temperature in Kelvin (300 K).

For liquid sources, the carbon input rate was calculated by converting the liquid injection rate [μL/min] from liquid form to mol/min as follows:

$$\begin{aligned}\text{carbonconcentration (mol/min)} &= \text{liquidsourceinputrate } (\mu\text{L/min}) \times (1\ \text{mL}/1000\ \mu\text{L}) \\ &\times \text{liquiddensity (g/mL)} \times (1/\text{molarmass (g/mol)}) \\ &\times \text{numberofcarbonatomspermolecule}\end{aligned}$$

Raman Spectroscopy. Raman spectroscopic characterization was performed using a Thermo-Electron Raman spectrometer with an excitation wavelength of 532 nm and a macroscopic sampling diameter of 0.3 mm.

Activation Energy Calculation. Activation energies were calculated by fitting the plots of the log of the CNT initial growth rate *versus* the inverse of the growth temperature with the exponential temperature dependence of the growth rate with the temperature, *i.e.*, IGR $\propto e^{(-E_a/kT)}$, where IGR is the initial growth rate, E_a is the activation energy, k is the Boltzmann constant, and T is the temperature.

Conflict of Interest: The authors declare no competing financial interest.

Acknowledgment. We acknowledge support from the Nanotechnology Program "Carbon Nanotube Capacitor Development Project" (2006−2011), by the New Energy and Industrial Technology Development Organization ("NEDO"). The authors wish to acknowledge A. Otsuka and J. Sato for their technical assistance.

REFERENCES AND NOTES

1. Nikolaev, P.; Bronikowski, M. J.; Bradley, R. K.; Rohmund, F.; Colbert, D. T.; Smith, K. A.; Smalley, R. E. Gas-Phase Catalytic Growth of Single-Walled Carbon Nanotubes from Carbon Monoxide. *Chem. Phys. Lett.* **1998**, *313*, 91.
2. Hata, K.; Futaba, D. N.; Mizuno, K.; Namai, T.; Yumura, M.; Iijima, S. Water-Assisted Highly Efficient Synthesis of Impurity-Free Single-Waited Carbon Nanotubes. *Science* **2004**, *306*, 1362–1365.
3. Zhong, G.; Iwasaki, T.; Robertson, J.; Kawarada, H. Growth Kinetics of 0.5 cm Vertically Aligned Single-Walled Carbon Nanotubes. *J. Phys. Chem. B* **2007**, *111*, 1907–1910.
4. Hart, A. J.; Slocum, A. H. Rapid Growth and Flow-Mediated Nucleation of Millimeter-Scale Aligned Carbon Nanotube Structures from a Thin-Film Catalyst. *J. Phys. Chem. B* **2006**, *110*, 8250–8257.
5. Kayastha, V. K.; Wu, S.; Moscatello, J.; Yap, Y. K. Synthesis of Vertically Aligned Single- and Double-Walled Carbon Nanotubes without Etching Agents. *J. Phys. Chem. C* **2007**, *111*, 10158–10161.
6. Hernadi, K.; Fonseca, A.; Nagy, J. B.; Bernaerts, D.; Lucas, A. Fe-Catalyzed Carbon Nanotube Formation. *Carbon* **1996**, *34*, 1249–1257.
7. Hasegawa, K.; Noda, S. Real-Time Monitoring of Millimeter-Tall Vertically Aligned Single-Walled Carbon Nanotube Growth on Combinatorial Catalyst Library. *Jpn. J. Appl. Phys* **2010**, *49*, 085104-1–085104-6.
8. Chakrabarti, S.; Gong, K.; Dai, L. Structural Evaluation along the Nanotube Length for Super-Long Vertically Aligned Double-Walled Carbon Nanotube Arrays. *J. Phys. Chem. C* **2008**, *112*, 8136.
9. Ebbesen, T. W.; Ajayan, P. M. Large-Scale Synthesis of Carbon Nanotubes. *Nature* **1992**, *358*, 220–222.
10. Thess, A.; Lee, R.; Nikolaev, P.; Dai, H.; Petit, P.; Robert, J.; Xu, C.; Lee, Y. H.; Kim, S. G.; Rinzler, A. G.; *et al.* Crystalline Ropes of Metallic Carbon Nanotubes. *Science* **1996**, *273*, 483–487.
11. Saito, T.; Ohshima, S.; Okazaki, T.; Ohmori, S.; Yumura, M.; Iijima, S. Selective Diameter Control of Single-Walled Carbon Nanotubes in the Gas-Phase Synthesis. *J. Nanosci. Nanotechnol.* **2008**, *8*, 6153–6157.
12. Moisala, A.; Nasibulin, A. G.; Brown, D. P.; Jiang, H.; Khriachtchev, L.; Kauppinen, E. I. Single-Walled Carbon Nanotube Synthesis Using Ferrocene and Iron Pentacarbonyl in a Laminar Flow Reactor. *Chem. Eng. Sci.* **2006**, *61*, 4393–4402.
13. Kimura, H.; Futaba, D. N.; Yumura, M.; Hata, K. Mutual Exclusivity in the Synthesis of High Crystallinity and High Yield Single-Walled Carbon Nanotubes. *J. Am. Chem. Soc.* **2012**, *134*, 9219–9224.
14. Harutyunyan, A. R.; Chen, G.; Paronyan, T. M.; Pigos, E. M.; Kuznetsov, O. A.; Hewaparakrama, K.; Kim, S. M.; Zakharov, D.; Stach, E. A.; Sumanasekera, G. U. Preferential Growth of Single-Walled Carbon Nanotubes with Metallic Conductivity. *Science* **2009**, *326*, 116–120.

15. Chiang, W. H.; Sankaran, R. M. Linking Catalyst Composition to Chirality Distributions of As-Grown Single-Walled Carbon Nanotubes by Tuning NixFe1-x Nanoparticles. *Nat. Mater. Lett.* **2009**, *8*, 882–886.
16. Hernadi, K.; Fonseca, A.; Nagy, J. B.; Siska, A.; Kiricsi, I. Production of Nanotubes by the Catalytic Decomposition of Different Carbon-Containing Compounds. *Appl. Catal. A* **2000**, *199*, 245–255.
17. Li, Q.; Yan, H.; Zhang, J.; Liu, Z. Effect of Hydrocarbons Precursors on the Formation of Carbon Nanotubes in Chemical Vapor Deposition. *Carbon* **2004**, *42*, 829–835.
18. Liu, Y. G.; Chen, X. H.; Yang, Z.; Pu, Y. X.; Yi, B. Synthesis of Aligned Carbon Nanotube with Straight-Chained Alkanes by Nebulization Method. *Trans. Nonferrous Met. Soc. China* **2010**, *20*, 1012–1016.
19. Chen, P.; Wang, P. F.; Lin, G. D.; Zhang, H. B.; Tsai, K. R. Carbon Nanotube Prepared by Catalytic Pyrolysis of Methane. *Chem. J. Chin. Univ.-Chin.* **1995**, *16*, 1783–1784.
20. Nikolaev, P.; Bronikowski, M. J.; Bradley, R. K.; Rohmund, F.; Colbert, D. T.; Smith, K. A.; Smalley, R. E. Gas-Phase Catalytic Growth of Single-Walled Carbon Nanotubes from Carbon Monoxide. *Chem. Phys. Lett.* **1999**, *313*, 91–97.
21. Murakami, Y.; Chiashi, S.; Miyauchi, Y.; Hu, M.; Ogura, M.; Okubo, T.; Maruyama, S. Growth of Vertically Aligned Single-Walled Carbon Nanotube Films on Quartz Substrates and their Optical Anisotropy. *Chem. Phys. Lett.* **2004**, *385*, 298–303.
22. Eres, G.; Kinkhabwala, A. A.; Cui, H.; Geohegan, D. B.; Puretzky, A. A.; Lowndes, D. H. Molecular Beam-Controlled Nucleation and Growth of Vertically Aligned Single-Wall Carbon Nanotube Arrays. *J. Phys. Chem. B* **2005**, *109*, 16684–16694.
23. Zhong, G.; Hofmann, S.; Yan, F.; Telg, H.; Warner, J. H.; Eder, D.; Thomsen, C.; Milne, W. I.; Robertson, J. Acetylene: A Key Growth Precursor for Single-Walled Carbon Nanotube Forests. *J. Phys. Chem. C* **2009**, *113*, 17321–17325.
24. Bronikowski, M. J. Longer Nanotubes at Lower Temperatures: The Influence of Effective Activation Energies on Carbon Nanotube Growth by Thermal Chemical Vapor Deposition. *J. Phys. Chem. C* **2007**, *111*, 17705–17712.
25. Hasegawa, K.; Noda, S. Millimeter-Tall Single-Walled Carbon Nanotubes Rapidly Grown with and without Water. *ACS Nano* **2011**, *5*, 975–984.
26. Futaba, D. N.; Hata, K.; Yamada, T.; Mizuno, K.; Yumura, M.; Iijima, S. Kinetics of Water-Assisted Single-Walled Carbon Nanotube Synthesis Revealed by a Time-Evolution Analysis. *Phys. Rev. Lett.* **2005**, *95*, 056104.
27. Yamada, T.; Maigne, A.; Yudasaka, M.; Mizuno, K.; Futaba, D. N.; Yumura, M.; Iijima, S.; Hata, K. Revealing the Secret of Water-Assisted Carbon Nanotube Synthesis by Microscopic Observation of the Interaction of Water on the Catalysts. *Nano Lett.* **2008**, *8*, 4288–4292.
28. Kimura,H.; Goto, J.; Yasuda,S.;Sakurai, S.; Yumura, M.; Futaba, D. N.; Hata, K. The Infinite Possible Growth Ambients that Support Single-Wall Carbon Nanotube Forest Growth (in preparation)
29. Yasuda, S.; Futaba, D. N.; Yumura, M.; Iijima, S.; Hata, K. Diagnostics and Growth Control of Single-Walled Carbon Nanotube Forests Using a Telecentric Optical System for *in-Situ* Height Monitoring. *Appl. Phys. Lett.* **2008**, *93*, 143115-1–3.
30. Yasuda, S.; Hiraoka, T.; Futaba, D. N.; Yamada, T.; Yumura, M.; Hata, K. Existence and Kinetics of Graphitic Carbonaceous Impurities in Carbon Nanotube Forests to Assess the Absolute Purity. *Nano Lett.* **2009**, *9*, 769–773.
31. Yasuda, S.; Futaba, D. N.; Yamada, T.; Satou, J.; Shibuya, A.; Takai, H.; Arakawa, K.; Yumura, M.; Hata, K. Improved and Large Area Single-Walled Carbon Nanotube Forest Growth by Controlling the Gas Flow Direction. *ACS Nano* **2009**, *3*, 4164–4170.
32. Yamada, T.; Namai, T.; Hata, K.; Futaba, D. N.; Mizuno, K.; Fan, J.; Yudasaka, M.; Yumura, M.; Iijima, S. Size-Selective Growth of Double-Walled Carbon Nanotube Forests from Engineered Iron Catalysts. *Nat. Nanotechnol.* **2006**, *1*, 131–136.
33. Zhao, B.; Futaba, D. N.; Yasuda, S.; Akoshima, M.; Yamada, T.; Hata, K. Exploring Advantages of Diverse Carbon Nanotube Forests with Tailored Structures Synthesized by Supergrowth from Engineered Catalysts. *ACS Nano* **2009**, *3*, 108–114.
34. Futaba, D. N.; Goto, J.; Yasuda, S.; Yamada, T.; Yumura, M.; Hata, K. A Background Level of Oxygen-Containing Aromatics for Synthetic Control of Carbon Nanotube Structure. *J. Am. Chem. Soc.* **2009**, *131*, 15992–15993.